

The investigation of cathode layer of Molten Carbonate Fuel Cell manufactured by using printing techniques

Jarosław Milewski^{a,*}, Arkadiusz Sieńko^c, Tomasz Wejrzanowski^b, Armen Jaworski^d, Łukasz Szablowski^a, Karol Ówieka^b, Artur Olszewski^c, Arkadiusz Szczęśniak^a, Jakub Skibiński^b, Ołaf Dybiński^a

^aWarsaw University of Technology, Faculty of Power and Aeronautical Engineering, Institute of Heat Engineering, 21/25 Nowowiejska Street, 00-665 Warsaw, Poland

^bWarsaw University of Technology, Faculty of Material Engineering, 141 Wołoska Street, 02-507 Warsaw, Poland

^cArkuszowa Drukarnia Offsetowa Lmtd., 40 Traugutta Street, 05-825 Grodzisk Maz., Poland

^dCIM-mes Projekt Lmtd., 125/127 Jerozolimskie Street, 02-017 Warsaw, Poland

Abstract

The paper presents an investigation into the three cathode layers for the Molten Carbonate Fuel Cell that were obtained by using printing techniques on various surfaces. The main differences during the manufacturing process were the substrates used when printing the layers: glass and two different sorts of paper. The cathodes were investigated at the theoretical and experimental level. To identify the influence of the substrate used we built a mathematical model of the fuel cell, in which the influence is expressed by the conductivity of the layer. The paper demonstrates the possibility of using printing techniques to manufacture Molten Carbonate Fuel Cell layers.

Introduction

The real benefits of fuel cell technology need to be marketed more effectively. As with all technical progress and developments, the introduction of fuel cells to the commercial market [1] follows completely different rules than in engineering practice [2]. 'Real' consumers expect 'real' products which offer added value, are easy to handle, last a long time (long enough) and offer value for money. This is often not understood by technology developers, who prefer to firmly believe in their technology and its benefits, forgetting that market customers need to be persuaded and convinced to spend their money. Often design overrides technology and the example of hand-held phones gives a good impression of how mediocre and overpriced technology can overcome any cost considerations if it 'hits the right keys' with consumers. Technology marketers have to start thinking from a consumer's perspective if fuel cells are to be successfully turned into products that sell by themselves. This also includes reassessing the key targets for achieving the all-important initial market success. In the context of politics this, for instance, involves the cost targets set for market entry and the conditions arranged for market incentives and

subsidy programs. It has to be acknowledged that current markets are biased towards the incumbent technologies and that a variety of hidden subsidies exist that are not recognized; for instance, the external costs of energy services that are borne by society, not by the technology users. Hydrogen based technologies are the one of the most promising projects due to the possibility of harnessing them to store power from renewable sources [3, 4]. Heat can be accumulated by using thermal storage [5, 6] and is easier to store than electricity in relative terms [7–9]. Water electrolysis [10–15] and steam reforming of methane are the most popular processes for generating hydrogen from electricity, but hydrogen can also be generated from organic waste [16]. Synthesis of artificial fuels is also an option for storing electricity in a chemical way [17–19] and very often requires hydrogen as a by-product in the process.

The fact is that fuel cell printing in itself is an innovation. This innovation however extends further, as it concerns a new way of soaking electrolyte into matrix, which shortens the time and energy intensity of manufacturing and reduces waste. It is planned to apply - for the first time - two devices simultaneously: an electrolyte filler and a large format printer. In this context, we have a combination of devices that present a novel technological barrier hitherto not crossed anywhere in the world.

Molten carbonate fuel cells have predicted future use for combined power and cooling purposes. Solid Oxide Fuel

*Corresponding author

Email addresses: milewski@itc.pw.edu.pl (Jarosław Milewski),
arkadiusz.sienko@ado.com.pl (Arkadiusz Sieńko),
lukasz.szablowski@itc.pw.edu.pl (Łukasz Szablowski)

Cells are the second promising area of technology here [20–22]. Both types of cell can directly utilize natural gas [23] due to their elevated operating temperature [24–28]. An interesting concept is presented in [29], where recovery of the waste heat produced in molten carbonate fuel cells is achieved through a thermoelectric generator and a thermoelectric cooler. Numerical calculations show that the power density and efficiency of the hybrid system are 3.4% and 4.0% larger than that of the stand-alone MCFC, respectively. The working principles of MCFC make it an ideal candidate technology for capturing carbon dioxide [30, 31] from fossil fuel power plants [32–34]. Theoretically, MCFC can also work in reversible mode [35] opening up the possibility of co-electrolysis carbon dioxide into synthetic fuels [36].

Printing is a popular technology in many technical fields in the world, as it is quite cheap and requires only limited consumption of materials and energy. The market is expecting technological advancements in printing in a vast scope ranging from the automotive industry and the military to advanced medicine. Should we be successful with our project, we will become leaders in the field, as our products will not only be technologically advanced due to their unique operating features, but also highly cost-competitive because of their lower manufacturing cost.

Table 1: Typical industrial priming process characteristics for different printing methods

Method	Line speed, m/s	Machine width, m	Calculated production capacity, m ² /h	Typical achievable printed layer thickness, μ
Gravure printing	20	2.4	130,000	2
Screen printing	2	1	7,200	100 .. 300
Flexography	10	1.5	54,000	5
Ink jet (industrial)	1	1	3,600	10
Offset printing	15	1.5	81,000	2

Several printing techniques such as flexography, screen printing, gravure printing and inkjet printing offer interesting opportunities in the manufacture of thin power sources. These processes give a wide variety of manufacturing methods that can be utilized in creating thin porous layers in a cost efficient way. Table 1 contains selected characteristics of different kinds of printing methods and parameters of the printed layers created by them.

Referring to Table 1 again, printing processes are mass manufacturing methods that have really high production capacities. The other advantage of printing processes is that they enable patterning. This means that it is relatively easy to tailor the shape of the printed layers to meet the requirements of different applications.

Different printing methods are used for different purposes in publication printing. For example, gravure printing is typically used for printing high quality magazines; offset print-

ing is used for printing newspapers; flexography for printing packages; inkjet for personalizing printed products; and screen printing for different kinds of specialty products such as posters or Braille. These different printing methods all reflect different kinds of demands, in terms of printing substrate and ink quality. For example, rotogravure printing is very sensitive to the smoothness of the printing substrate whereas flexography can be used for rougher substrates.

In rotogravure printing the printing ink is transferred to printing substrates by engraved cups in the metallic printing cylinder in a nip that is formed between the printing cylinder and backup roll. With rotogravure it is possible to achieve very good resolution, high print quality and extremely high production capacity. The inks used in rotogravure have very low viscosity.

Flexography printing works, in principle, like a stamp. Printing ink is lifted with an engraved anilox roll to a patterned printing cylinder made from polymer materials. The ink is then transferred from the printing plate to the printing substrate. The amount of ink transferred is mainly controlled by the anilox roll parameters. The inks in flexography have higher viscosity than rotogravure inks.

Offset printing is another high output printing method. It has a rather complicated ink transfer process and it is, therefore, not widely used in the printing of active materials. Tailoring the active inks to be suitable for offset is also demanding. Offset printing is a lithographic printing method in which ink is fed to a separate ('offset') printing blanket through an impression cylinder. The printing image is formed in the impression cylinder by areas that have different surface chemical features. Printing ink wets areas in the impression cylinder that have compatible surface energy with the ink and an image is formed on these areas. Offset printing is the most widely used printing method in publication printing, because it has good quality, high production capacity and is relatively quickly prepared for starting the production process.

Screen printing is a method in which the ink is forced through a patterned wire to the printing substrate. It is relatively easy to adopt because it has virtually no demands as regards the quality of the printing substrate. It can also be used to create extremely thick printed layers, which is the reason why it is used in the printing of many different kinds of functional inks. Moreover, screen printing allows the use of highly viscous inks, which extends its scope of applicability as many functional inks have an extremely high ratio of dry matter.

Printing can also be used in combination with other manufacturing techniques such as laminating and heat sealing. For example, printable anodes and cathodes could be printed with a separator membrane laminated between them. However, printing machines are usually unsuitable for printing fuel or solar cells without some tailoring. Typically, a single machine does not have all the necessary unit operations installed in it. Additionally, printing the cells requires somewhat different characteristics. In the case of publication printing, the appearance of the printed image is the most crucial feature, whereas for printed cell components the re-

quirements are more complex and include, apart from the surface features, the specific volume structure to satisfy certain thickness thresholds.

The various printing techniques do not lend themselves to the full range of fuel cells, because they require various structures that need to be manufactured by printing. For example, solid oxide fuel cells [37–45] and molten carbonate fuel cells [46] require thick anode and cathode layers to achieve high power densities [47, 48]. On the other hand, printed solar cells require thin, pinhole free and very uniform anode and cathode layers for the cell. This means that different types of power sources need different printing methods for optimum performance. For instance solid oxide fuel cells (SOFC) can be manufactured by a silk screen process, which creates thick layers, while solar cells are optimally manufactured by rotogravure printing, which is able to create extremely thin layers [49].

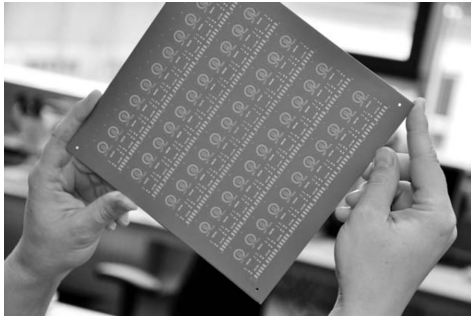


Figure 1: Large size (200×200 mm), low-temperature co-fired ceramic substrate with mass produced, highly repetitive, ceramic multilayer substrate size is the industry standard

Multilayer ceramics [50], in principle, may be compared to multilayer printed circuit board (PCB) technology. Individual layers of unfired, ‘green’ ceramics are modified to carry a specific functionality (e.g., electric conductivity) and laminated afterwards. Upon lamination, inter-layer connections are formed. After a final sintering step, the ceramic ‘PCB’ is ready for component assembly (Figure 1). For the cathode layer of the planar Solid Oxide Fuel Cell, slurry coating is done through a screen-printing process [51] and the final thicknesses of the cathode layers are between 150 and 200 microns. [52] reports the results obtained in the characterization of electrocatalysts prepared by screen printing and chemical synthesis. A homogenous paste of transition metal carbonyl compounds was prepared in this way. Once the paste was prepared it was printed onto a porous carbon substrate. The electrocatalytic activity of the compounds was studied.

[53] presents a method of using inkjet printing to deposit catalyst materials onto gas diffusion layers that are made into membrane electrode assemblies for a polymer electrolyte fuel cell. They claim that ink deposition methods such as spray painting or screen printing are not well suited for ultra low loading. The inkjet printing method can be used to deposit smaller volumes of water based catalyst ink solutions with good precision provided the solution properties are com-

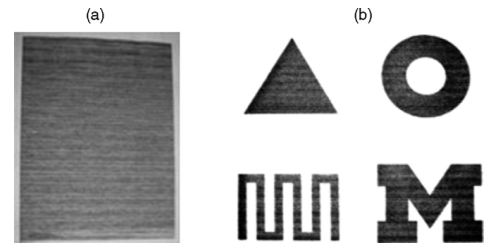


Figure 2: Illustration of successfully printed catalyst layers using the IJP method (a and b) [53]

patible with the cartridge design. By optimizing dispersion of the ink solution they showed this technique can be successfully used with catalysts supported on different carbon black (see Fig. 2). Paper [54] reviews additive manufacturing processes in research and development of fuel cell components, such as synthesizing and prototyping new materials for fuel cell components, fuel cell system design and prototyping, designing well sealed fuel cells, bridging from fuel cell design to manufacturing tooling, etc. The studies [55, 56] focus on the rheology of screen printing inks for the fabrication of porous composite Solid Oxide Fuel Cell anodes. Inks with 1 .. 3 wt% binder were suitable for screen printing, but inks with higher binder content were tacky and difficult to print. A method for producing continuous catalyst layers on substrate materials by gravure printing with the aid of catalyst-containing inks is shown in [57], where a printing plate is used which has at least one print image with an interrupted line screen whose longitudinal lines are arranged at an angle of front 10 to 80° relative to the printing direction. Preferably, the print images have dip volumes in the range from 100 to 300 ml/m². The catalyst layers produced are cohesive and continuous and have dry layer thicknesses in the range of 1 to 20 μm, preferably in the range of 2 to 15 nm.

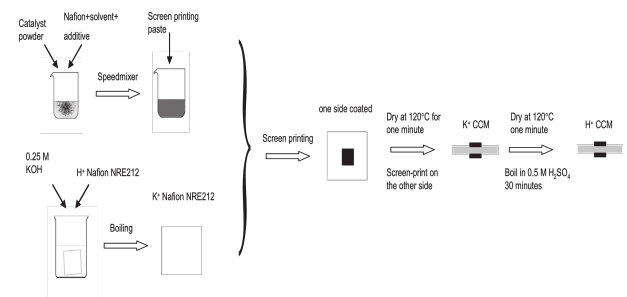


Figure 3: Schematic of the CCM-MEA preparation procedure using direct screen printing[58]

A catalyst coated membrane technique based on a novel screen printing paste was proposed in [58]. The complete procedure for the fabricated membrane with the direct screen printing method was illustrated in Fig. 3. Then the screen printing paste was applied to both sides of the membrane step by step with a screen printer. The article [59] presents a review of screen-printing inks for the fabrication of Solid Oxide Fuel Cell components by screen printing. In this context, it covers a vast property of screen-printing inks and screen-

printer parameters, which determine the quality and performance of the screen-printed films. A novel additive manufacturing approach incorporating selective laser sintering [60] was used to fabricate a non-carbon-based GDL directly from a 3D printing technique to circumvent electrochemical degradation of carbon-based gas diffusion layer, which is an integral constituent in a Polymer Exchange Membrane Fuel Cell stack.

Based on the literature review presented, it seems that printing techniques were never previously used for manufacturing Molten Carbonate Fuel Cell components. Thus, in this paper we made an attempt to use the techniques to manufacture the cathode layer of Molten Carbonate Fuel Cells and investigated the role of the support [61] on which the layer is printed.

Theory

Generally speaking, MCFC works as a membrane that is a preamble for carbonate ions (CO_3^-), which are composed by one molecule of carbon dioxide and a half molecule of oxygen. This means that the voltage of MCFC depends on the partial pressures of carbon dioxide and oxygen at both its sides (anode and cathode) and is defined by the following equation:

$$E_{\max} = \frac{R \cdot T \cdot p_{\text{CO}_{2,c}}^2 \cdot p_{\text{O}_{2,c}}}{4 \cdot F \cdot p_{\text{CO}_{2,a}}^2 \cdot p_{\text{O}_{2,a}}} \quad (1)$$

where: p —partial pressure, bar; F —Faraday constant, C/mol; R —universal gas constant, J/mol/K.

MCFC voltage depends on four partial pressures, two carbon dioxide and two oxygen between cathode and anode. A mixture of oxygen and carbon dioxide is fed to the cathode, which gives adequate pressure ratios. On the anode side, the fuel reacts with oxygen and carbon dioxide is released to the anode stream. Anode gases partial pressures depend on the current operational conditions of the fuel cell. Additionally, to avoid fast electrolyte evaporation, carbon dioxide is also supplied at the anode inlet. Several factors impact fuel cell voltage and they are agglomerated in the mathematical model. In contrast to semi-empirical models [62–64], the impact of electrode parameters on MCFC behavior is clearly described by the Reduced Order model [65, 66]. The equation for cell voltage is defined as:

$$E_{\text{MCFC}} = \frac{E_{\max} - \eta_f \cdot i_{\max} \cdot r_1}{\frac{r_1}{r_2} \cdot (1 - \eta_f) + 1} \quad (2)$$

MCFC voltage is described by a number of factors which have physical explanations: E_{\max} —maximum voltage defined by maximum work of isothermal process; η_f —fuel utilization factor defined by current working conditions of the cell; i_{\max} —maximum current density defined by quantity of delivered fuel or oxidant; r_1 —area specific internal ionic resistance (ASIIIR) defined by permeability of electrolyte (entire fuel cell) for carbonate ions; and r_1 —area specific inter-

nal electronic resistance (ASIER) defined by electric conductance of the molten electrolyte (entire fuel cell).

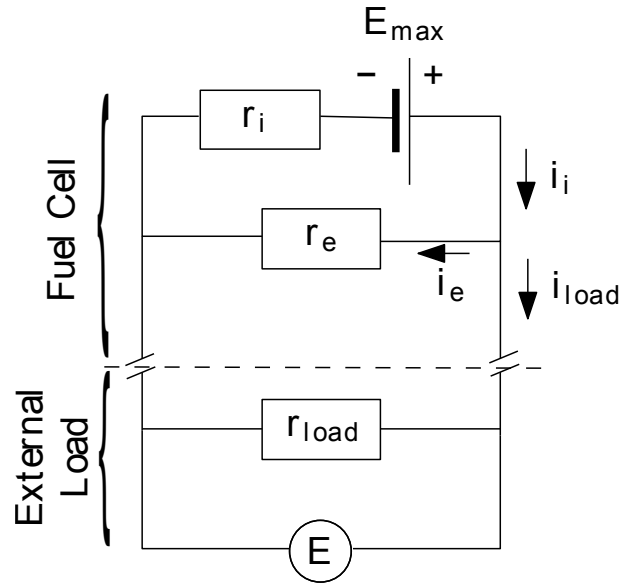


Figure 4: Basic equivalent electric circuit of Molten Carbonate Fuel Cell

Eq. 2 based on the equivalent electric circuit as shown in Fig. 4, in its basic form. To investigate the influence of electrodes, the circuit needs to be modified by adding additional resistances in the places linked to the electrodes.

The influence of electrode parameters (materials, porosity, etc) is included in the area specific resistances—see Fig. 5. The electrodes' resistances can be agglomerated as resistance r_3 :

$$r_3 = r_a + r_c + r_{\text{other}} \quad (3)$$

Thus the basic equation is modified to reflect the changes and takes the following form:

$$E_{\text{MCFC}} = \frac{E_{\max} - \eta \cdot i_{\max} \cdot r_1 + \frac{r_3}{r_2} \cdot \eta \cdot (E_{\max} - i_{\max} \cdot (r_1 + r_2))}{\frac{r_1}{r_2} \cdot (1 - \eta) + 1} \quad (4)$$

Fuel cell voltage depends on the cathode parameters which are expressed by r_c (see Eq. 3). The area specific resistance depends on the thickness of the electrode and its conductivity:

$$r_c = \frac{\delta_c}{\sigma_c} \quad (5)$$

where: δ —thickness, cm; σ —conductivity, S/cm.

The thickness of the layer is given, thus the only function we are looking for is conductivity, which mainly depends on operational temperature and can be expressed by the Arrhenius equation:

$$\sigma_c = A_0 \cdot e^{\frac{-E_{\text{act}}}{RT}} \quad (6)$$

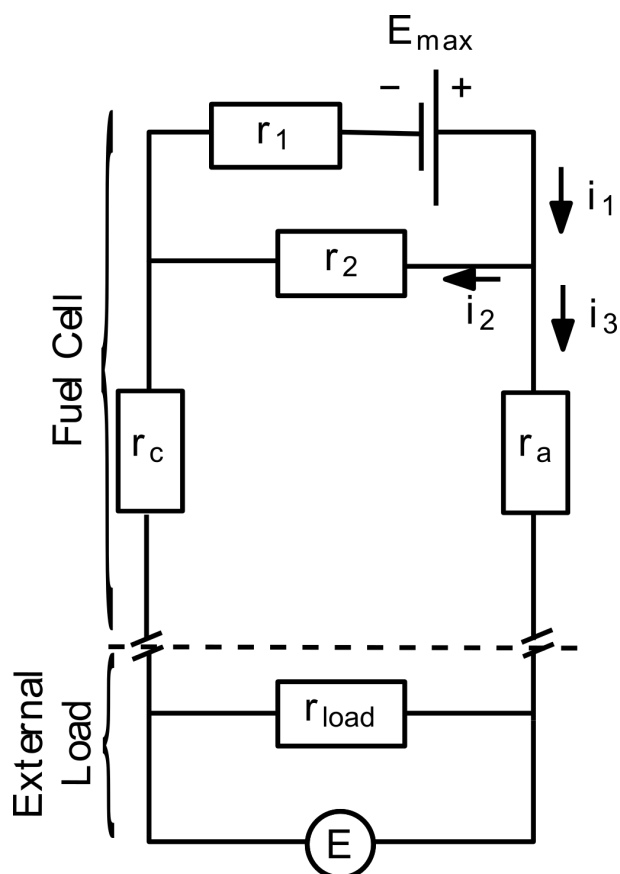


Figure 5: Equivalent electric circuit of Molten Carbonate Fuel Cell with additional resistances for modeling the electrodes

where: T —temperature, K; A_0 —preexponential constant, S/cm; E_{act} —energy activation, kJ/kmol; R —universal gas constant, 8.315 kJ/kmol/K.

The task is to find these two coefficients: A_0 and E_{act} , the second one mostly describes the influence of temperature. To this end, we performed a few sets of experiments and entered the results into an Excel spreadsheet containing all the provided equations. Then we calculated the error between measured and modeled values for each experimental points. The errors are defined as the square of the difference between the values obtained from the model and the experiments. Excel has a built-in tool called Solver, which can be used for optimizing (maximizing or minimizing) a selected objective function. We tasked Solver with minimizing the sum of errors for all experimental points by changing those two parameters (A_0 and E_{act}). By doing this, we can estimate the values of conductivity of the cathode layer varied with change of the substrate used during the manufacturing process (printing).

Preparation of fuel cell layers

The whole process of preparing Molten Carbonate Fuel Cell components is shown in Fig. 6. The process consists of a few steps, which are indicated in general terms. Slurry

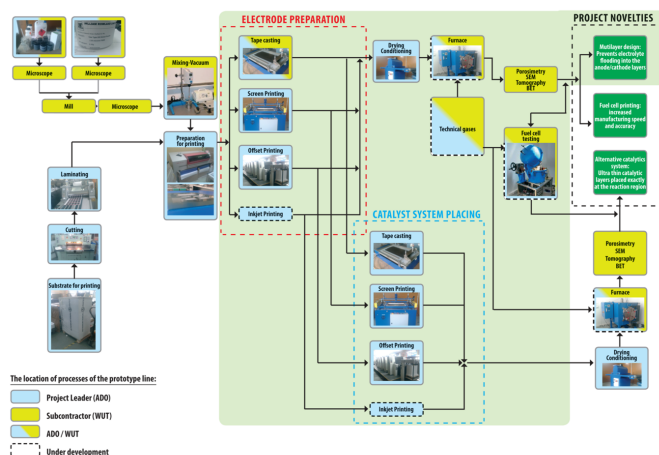


Figure 6: The process of printing Molten Carbonate Fuel Cell components

preparation for screen printing is generally the same as for the tape casting technique. The whole process of printing the MCFC is divided into several sections. The first two steps involve preparation of the slurries and substrates. Then the substrate slurries are placed on the substrates by various techniques. Tape casting is also used for obtaining the reference layers that can be used for comparing the layers manufactured by other techniques. Sintering takes place after the slurries are placed on the substrate. The sintering process depends on the type of electrode (anode, cathode) and substrate (glass, paper). Generally speaking, the sintering process is done in a multi-step procedure in which both the temperature and process environment are changed. Final layers are investigated according to their material properties (porosity, structure, surfaces) and are tested in the fuel cell laboratory stand against the reference values.

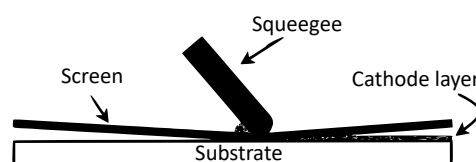


Figure 7: Schematic diagrams of the screen printing technique [67]

The description of the screen printing process depicted in Fig. 7 follows [67]. During deposition, the screen is placed a few millimeters above the surface of the substrate. Upon loading the cathode slurry solution onto the screen, a rubber “squeegee” is then swept with a velocity of several centimeters per second across the surface of the screen, with contact being made momentarily between it and the substrate. At this point, solution flows from the screen to the surface of the substrate. As the squeegee then passes over a region, the screen separates from the substrate, leaving behind a solution that dries to yield a continuous film.

Fig. 8 presents real the screen printing process of MCFC cathode layer, where: 1—squeegee, 2—slurry, 3—screen surface, 4—printed cathode layer, 5—substrate.

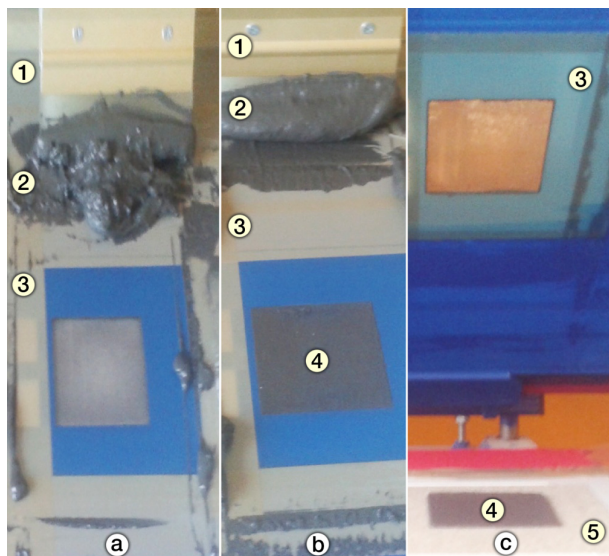


Figure 8: Actual screen printing process of the MCFC cathode layer: (a) the stencil ready to be printed; (b) view of the screen after printing run; (c) view of the reverse side of the screen after printing



Figure 9: Molten Carbonate Fuel Cell cathode layers screen-printed on various substrates

The final results of the screen printed cathodes are presented in Fig. 9. The same slurry was placed on different substrates.

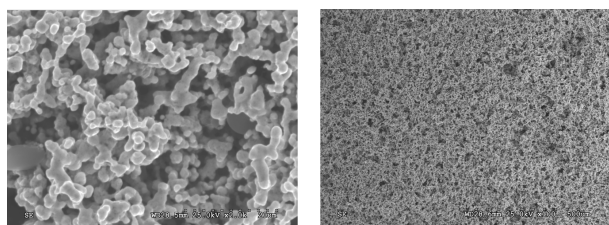


Figure 10: High (left) and low magnification (right) SEM image of porous MCFC cathode fabricated by screen printing

The printed cathodes were investigated by Spectroscopy Electron Microscopy imaging for low and high resolution imaging. The structure is very porous, with properly sintered

particles of nickel powder.

Experimental investigation



Figure 11: Stand for testing high-temperature fuel cells at Warsaw University of Technology

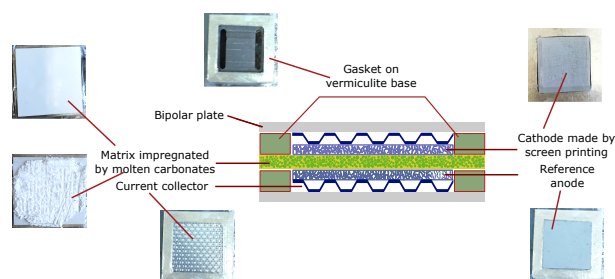


Figure 12: Diagram of the cathode test stand for carbonate fuel cells

Experimental tests were carried out on the test bench for fuel cells, the lab stand is fully automatic with a pressurized vessel used for compressing the cell. The cells can also be tested at pressurized conditions if necessary, see Fig. 11. The tests were carried out in single cell architecture, where the bottom layer was made up of a reference anode (made

by tape casting), a 316 stainless steel current collector and a ceramic matrix impregnated by molten electrolyte, and then the cathode made by the printing technique; for details see Fig. 12.

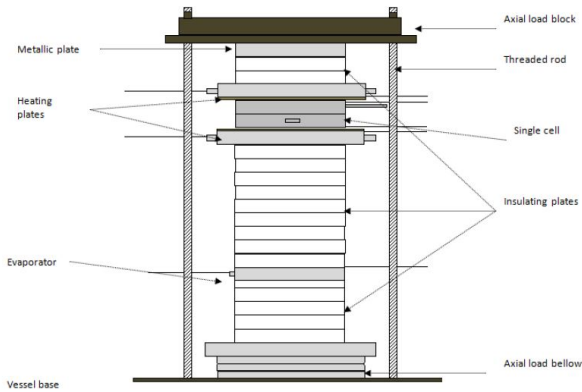


Figure 13: Single fuel cell position in the experimental station

The single cell together with housing was compressed in the lab stand by using a pressurized cylinder at the bottom of the experimental station (Fig. 13). The pair of heaters are used for heating up the cell during the start-up procedure as well as maintaining the desired temperature during experiments. Anode sizes used for the tests were 5 x 5 cm, cathode 4.5 x 4.5 cm and the matrix 7 x 7 cm.

Table 2: The compositions of gases supplied to fuel cells

Flows, NI/h	Side	Hydrogen	Carbon Dioxide	Air
Max Flows	Anode	20.33	5.09	–
	Cathode	–	20	46.5
Reference Point	Anode	3.36	0.82	–
	Cathode	–	3.25	7.80
No CO ₂ at anode	Anode	3.36	–	–
	Cathode	–	3.25	7.80

The fuel cells were tested with three various gas compositions indicated as Reference Point (RP), Maximum Flows (MaxFlow), and Reference Point without supplying carbon dioxide into the anode inlet. All those compositions are presented in Table 2. We habitually make use of the reference point for all experiments, to compare various solutions between cells. The maximum flow conditions are used to minimize the effect of the fuel utilization factor on fuel cell characteristics. Carbon dioxide has to be supplied at the cathode side to comply with fuel cell working principles. On the other hand, CO₂ at the anode inlet is supplied for other reasons (electrolyte stability) and decreases open circuit voltage (OCV); see Eq. 1. Since the cathode layer may influence the OCV as well, we did the tests without carbon dioxide at the anode inlet to judge the impact.

The aim of the work carried out is to verify the due operation of the manufacturing line based on the innovative technological process on an industrial scale and its selected configuration (binders, process speed, powder granulation, etc.). In order to investigate the validity of the manufacturing

line and the innovative process, the operation of individual system components and of the whole system is examined. Any dysfunctional parts of the process are eliminated by industrial research performed by a subcontractor, resulting in modifications to the process and materials provided in order to improve functioning. As a result of these actions, improvements are achieved in terms of tested and tailored manufacturing processes for cost-effective power source components.

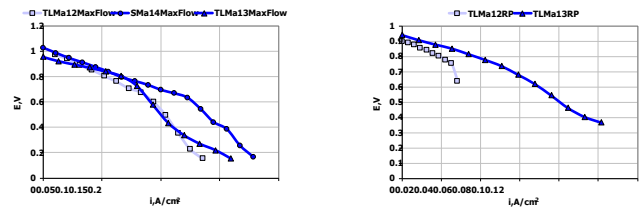


Figure 14: Comparison of current-voltage curves for fuel cells containing printed cathodes 1708-TLMa12, 1708-TLMa13 and 1708-SMa14 for maximum flows (a) and reference flows (b)

Validity of the innovative process is verified by experimental industrial research regarding manufactured components, carried out by a subcontractor. The results are used to select, develop and install an innovative manufacturing line for cost-effective power source components.

Figure 14 presents a comparison of current-voltage curves for cells containing printed cathodes 1708-TLMa12, 1708-TLMa13 and 1708-SMa14 for maximum flows (MaxFlow). Figure 15 shows a comparison of current-voltage curves for cells containing printed cathodes 1708-TLMa12, 1708-TLMa13 and 1708-SMa14 for reference flows (RP).

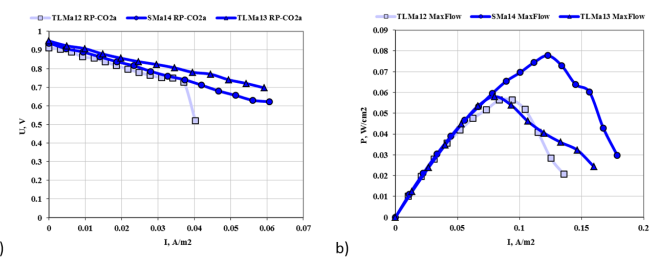


Figure 15: Comparison of current-voltage curves for cells containing printed cathodes 1708-TLMa12, 1708-TLMa13 and 1708-SMa14 for reference flows, but without CO₂ on the anode (a); comparison of power density versus current density for cells containing printed cathodes 1708-TLMa12, 1708-TLMa13 and 1708-SMa14 for maximum flows (b)

Comparison of current-voltage curves for cells containing printed cathodes 1708-TLMa12, 1708-TLMa13 and 1708-SMa14 for reference flows, but without CO₂ on the cell anode (RP-CO₂a) is shown in Fig. 15a. In Fig. 15b, a comparison of power density vs. current density has been shown for cells containing printed cathodes 1708-TLMa12, 1708-TLMa13 and 1708-SMa14 for maximum flows (MaxFlow).

A comparison of power density as a function of current density for cells containing printed cathodes 1708-TLMa12 and 1708-TLMa13 for reference flows (RP) is shown in

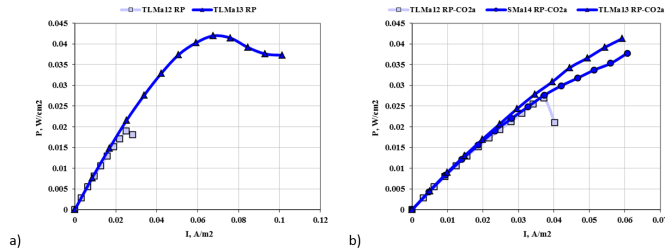


Figure 16: Comparison of power density vs. current density for cells containing printed cathodes 1708-TLMA12 and 1708-TLMA13 for reference flows (a); comparison of power density versus current density for cells containing printed cathodes 1708-TLMA12, 1708-TLMA13 and 1708-SMA14 for reference flows, but without CO₂ at anode inlet (b)

Fig. 16a. A comparison of power density vs. current density for cells containing printed cathodes 1708-TLMA12, 1708-TLMA13 and 1708-SMA14 for reference flows, but without CO₂ on the cell anode (RP-CO₂a), can be seen in Fig. 16b.

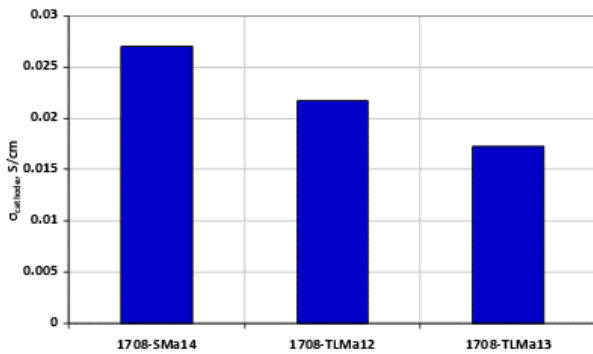


Figure 17: Estimated conductivity values of the tested cathode layers

Based on experimental data, the influence of a given cathodic layer on fuel cell performance was tested. The results of approximation of experimental data using a mathematical model are used to estimate the conductivity of given layers. The results are summarized in Fig. 17.

Discussion

For the three investigated substrates, the greatest cathode conductivity was achieved for a glass substrate, whereas the lowest was for a paper. This can be caused by the sintering process, during the course of which paper can leave carbon particles on cathode surface. The cathodes were sintered with a nitrogen/hydrogen atmosphere, thus the carbon can remain, whereas glass is neutral for that phenomena.

Both cathodes printed on paper had comparable power densities for reference conditions without CO₂ at the anode (they would probably also have comparable power densities for reference conditions).

The poorer performance of the fuel cell containing the paper printed cathode could be due to the lower average op-

erating temperature compared to the other two cells. Nevertheless, the mathematical model of the fuel cell takes into account the influence of temperature on performance, eliminating this disruption, and was used to assess this phenomenon.

The results of the experiments showed that printing methods can be used to obtain working elements of molten carbonate cells with similar conductivity of cathodes (σ , S/cm). The best results were obtained for a cathode made by screen printing on a glass substrate.

Conclusions

The paper presents an investigation into three various cathode layers for a Molten Carbonate Fuel Cell obtained by using printing techniques. The main difference during the manufacturing process was the substrate used when printing the layers: glass and two different sorts of paper. We demonstrated that mass scale printing techniques are capable of manufacturing Molten Carbonate Fuel Cell elements. The effects of the three different substrates were investigated from the cathode layer conductivity point of view, and the greatest conductivity was achieved by the cathode which was produced by screen printing on a glass substrate. The cathodes were investigated both experimentally and theoretically. Based on experimental data, the influence of a given cathodic layer on the fuel cell performance was tested and the results of approximation of experimental data using a mathematical model were used to estimate the conductivity of given layers. The differences between investigated substrates are not spectacular. The tests were performed for various temperatures and various gas compositions to identify the impact of the cathode used (reference conditions, maximum flows and no CO₂ at the anode).

Acknowledgments

The project is co-financed by the Polish National Center for Research and Development of Operational Programme Smart Growth, INNOCHEM sectoral programme granted by agreement number POIR.01.02.00-00-0045/16.

References

- [1] R. Roshandel, F. Golzar, M. Astaneh, Technical economic and environmental optimization of combined heat and power systems based on solid oxide fuel cell for a greenhouse case study, *Energy Conversion and Management* 164 (2018) 144–156.
- [2] J. Yan, F. Sun, S. Chou, U. Desideri, H. Li, P. Campana, R. Xiong, Transformative innovations for a sustainable future – Part III, *Applied Energy* 227 (2018) 1–6.
- [3] J. Kotowicz, L. Bartela, K. Dubiel-Jurgaś, Analysis of Energy Storage System with Distributed Hydrogen Production and Gas Turbine, *Archives of Thermodynamics* 38 (4) (2017) 65–87.
- [4] J. G. G. Clúa, R. J. Mantz, H. D. Battista, Optimal sizing of a grid-assisted wind-hydrogen system, *Energy Conversion and Management* 166 (2018) 402–408.
- [5] M. Leško, W. Bujalski, Modeling of District Heating Networks for the Purpose of Operational Optimization with Thermal Energy Storage, *Archives of Thermodynamics* 38 (4) (2017) 139–163.

- [6] R. Bartnik, Z. Buryń, A. Hnydiuk-Stefan, A. Juszcak, Methodology and a Continuous Time Mathematical Model for Selecting the Optimum Capacity of a Heat Accumulator Integrated with a CHP Plant, *Energies* 11 (5) (2018) 1240.
- [7] L. Szablowski, P. Krawczyk, K. Badyda, S. Karellas, E. Kakaras, W. Bujalski, Energy and exergy analysis of adiabatic compressed air energy storage system, *Energy* 138 (2017) 12–18.
- [8] A. Chmielewski, P. Piorkowski, K. Bogdzinski, P. Szulim, R. Guminski, Test bench and model research of hybrid energy storage, *JOURNAL OF POWER TECHNOLOGIES* 97 (5) (2017) 406–415.
- [9] J. Yu, J. Fu, F. Guo, Y. Xie, Automatic testing system to evaluate the energy efficiency of electric storage water heaters, *Measurement and Control* 51 (7-8) (2018) 223–234.
- [10] S. Fukuzumi, Y.-M. Lee, W. Nam, Fuel Production from Seawater and Fuel Cells Using Seawater, *ChemSusChem* 10 (22) (2017) 4264–4276.
- [11] Y. Chen, F. Mojica, G. Li, P.-Y. A. Chuang, Experimental study and analytical modeling of an alkaline water electrolysis cell, *International Journal of Energy Research* 41 (14) (2017) 2365–2373.
- [12] B. Hu, A. N. Aphale, C. Liang, S. J. Heo, M. A. Uddin, P. Singh, Carbon Tolerant Double Site Doped Perovskite Cathodes for High-Temperature Electrolysis Cells, *ECS Transactions* 78 (1) (2017) 3257–3265.
- [13] S. Lepszy, T. Chmielniak, P. Monka, Storage system for electricity obtained from wind power plants using underground hydrogen reservoir, *JOURNAL OF POWER TECHNOLOGIES* 97 (1) (2017) 61–68.
- [14] C. Seibel, J.-W. Kuhlmann, Dynamic Water Electrolysis in Cross-Sectoral Processes, *Chemie Ingenieur Technik* 90 (10) (2018) 1430–1436.
- [15] L. Barelli, G. Bidini, G. Cinti, Air variation in SOE: Stack experimental study, *International Journal of Hydrogen Energy* 43 (26) (2018) 11655–11662.
- [16] A. Z. Senseni, F. Meshkani, S. M. S. Fattahi, M. Rezaei, A theoretical and experimental study of glycerol steam reforming over Rh/MgAl₂O₄ catalysts, *Energy Conversion and Management* 154 (2017) 127–137.
- [17] Q. Zhuang, P. Geddis, A. Runstedtler, B. Clements, An integrated natural gas power cycle using hydrogen and carbon fuel cells, *Fuel* 209 (2017) 76–84.
- [18] G. Leonzio, State of art and perspectives about the production of methanol dimethyl ether and syngas by carbon dioxide hydrogenation, *Journal of CO₂ Utilization* 27 (2018) 326–354.
- [19] F. B. Juangsa, L. A. Prananto, Z. Mufrodi, A. Budiman, T. Oda, M. Aziz, Highly energy-efficient combination of dehydrogenation of methylcyclohexane and hydrogen-based power generation, *Applied Energy* 226 (2018) 31–38.
- [20] V. Subotić, B. Stoeckl, V. Lawlor, J. Strasser, H. Schroettner, C. Hochenauer, Towards a practical tool for online monitoring of solid oxide fuel cell operation: An experimental study and application of advanced data analysis approaches, *Applied Energy* 222 (2018) 748–761.
- [21] A. H. Davoodi, M. R. Pishvaie, Plant-Wide Control of an Integrated Molten Carbonate Fuel Cell Plant, *Journal of Electrochemical Energy Conversion and Storage* 15 (2) (2018) 021005.
- [22] M. A. Azizi, J. Brouwer, Progress in solid oxide fuel cell-gas turbine hybrid power systems: System design and analysis transient operation, controls and optimization, *Applied Energy* 215 (2018) 237–289.
- [23] M. Recalde, T. Woudstra, P. Aravind, Renewed sanitation technology: A highly efficient faecal-sludge gasification–solid oxide fuel cell power plant, *Applied Energy* 222 (2018) 515–529.
- [24] J. Badur, M. Lemański, T. Kowalczyk, P. Ziółkowski, S. Kornet, Zero-dimensional robust model of an SOFC with internal reforming for hybrid energy cycles, *Energy* 158 (2018) 128–138.
- [25] P. Jienkulsawad, D. Saebea, Y. Patcharavorachot, S. Kheawhom, A. Arpornwichanop, Analysis of a solid oxide fuel cell and a molten carbonate fuel cell integrated system with different configurations, *International Journal of Hydrogen Energy* 43 (2) (2018) 932–942.
- [26] I. Baikov, O. Smorodova, S. Kitaev, I. Yerilin, Temperature influence on internal reforming and methane direct oxidation in solid oxide fuel cells, *Nanotechnologies in Construction: A Scientific Internet-Journal* 10 (4) (2018) 120–137.
- [27] M. Dillig, T. Plankenbühler, J. Karl, Thermal effects of planar high temperature heat pipes in solid oxide cell stacks operated with internal methane reforming, *Journal of Power Sources* 373 (2018) 139–149.
- [28] S. Campanella, M. Bracconi, A. Donazzi, A fast regression model for the interpretation of electrochemical impedance spectra of Intermediate Temperature Solid Oxide Fuel Cells, *Journal of Electroanalytical Chemistry* 823 (2018) 697–712.
- [29] M. Wu, H. Zhang, T. Liao, Performance assessment of an integrated molten carbonate fuel cell-thermoelectric devices hybrid system for combined power and cooling purposes, *International Journal of Hydrogen Energy* 42 (51) (2017) 30156–30165.
- [30] W. M. Budzianowski, Assessment of Thermodynamic Efficiency of Carbon Dioxide Separation in Capture Plants by Using Gas–Liquid Absorption, in: *Green Energy and Technology*, Springer International Publishing, 2016, pp. 13–26.
- [31] D. Bonaventura, R. Chacartegui, J. Valverde, J. Becerra, C. Ortiz, J. Lizana, Dry carbonate process for CO₂ capture and storage: Integration with solar thermal power, *Renewable and Sustainable Energy Reviews* 82 (2018) 1796–1812.
- [32] R. Carapellucci, R. Cipollone, D. D. Battista, Modeling and characterization of molten carbonate fuel cell for electricity generation and carbon dioxide capture, *Energy Procedia* 126 (2017) 477–484.
- [33] S. K. Das, Towards enhancement of carbon capture by Molten Carbonate Fuel Cell through controlled thermodiffusion, *International Journal of Heat and Mass Transfer* 127 (2018) 296–302.
- [34] Q. Zhuang, P. Geddis, A. Runstedtler, B. Clements, A power cycle of natural gas decarbonization and dual fuel cells with inherent 100% carbon capture, *International Journal of Hydrogen Energy* 43 (39) (2018) 18444–18451.
- [35] J. P. Perez-Trujillo, F. Elizalde-Blancas, M. D. Pietra, S. J. McPhail, A numerical and experimental comparison of a single reversible molten carbonate cell operating in fuel cell mode and electrolysis mode, *Applied Energy* 226 (2018) 1037–1055.
- [36] P. Fragiaco, G. D. Lorenzo, O. Corigliano, Performance Analysis of an Intermediate Temperature Solid Oxide Electrolyzer Test Bench under a CO₂-H₂O Feed Stream, *Energies* 11 (9) (2018) 2276.
- [37] and, Dynamic Analysis of Load Operations of Two-Stage SOFC Stacks Power Generation System, *Energies* 10 (12) (2017) 2103.
- [38] J. Kupecki, K. Motyliński, M. Skrzypekiewicz, M. Wierzbicki, Y. Naumovich, Preliminary Electrochemical Characterization of Anode Supported Solid Oxide Cell (AS-SOC) Produced in the Institute of Power Engineering Operated in Electrolysis Mode (SOEC), *Archives of Thermodynamics* 38 (4) (2017) 53–63.
- [39] Y. Zheng, Y. Luo, Y. Shi, N. Cai, Dynamic Processes of Mode Switching in Reversible Solid Oxide Fuel Cells, *Journal of Energy Engineering* 143 (6) (2017) 04017057.
- [40] O. Siddiqui, I. Dincer, Analysis and performance assessment of a new solar-based multigeneration system integrated with ammonia fuel cell and solid oxide fuel cell-gas turbine combined cycle, *Journal of Power Sources* 370 (2017) 138–154.
- [41] N. Danilov, A. Tarutin, J. Lyagaeva, E. Pikalova, A. Murashkina, D. Medvedev, M. Patrakeev, A. Demin, Affinity of YBaCo₄O_{7+δ}-based layered cobaltites with protonic conductors of cerate-zirconate family, *Ceramics International* 43 (17) (2017) 15418–15423.
- [42] M. L. Ferrari, A. Sorce, A. F. Massardo, Hardware-in-the-Loop Operations With an Emulator Rig for SOFC Hybrid Systems, in: *Volume 3: Coal Biomass and Alternative Fuels, Cycle Innovations, Electric Power, Industrial and Cogeneration Applications, Organic Rankine Cycle Power Systems*, ASME, 2017.
- [43] K. Motyliński, Y. Naumovich, Numerical model for evaluation of the effects of carbon deposition on the performance of 1 kW SOFC stack – a proposal, *E3S Web of Conferences* 14 (2017) 01043.
- [44] R. Ma, C. Liu, E. Breaz, P. Briois, F. Gao, Numerical stiffness study of multi-physical solid oxide fuel cell model for real-time simulation applications, *Applied Energy* 226 (2018) 570–581.
- [45] Z. Ye, X. Zhang, W. Li, G. Su, J. Chen, Optimum operation states and parametric selection criteria of a high temperature fuel cell-thermoradiative cell system, *Energy Conversion and Management* 173 (2018) 470–475.
- [46] G. Accardo, D. Frattini, S. P. Yoon, H. C. Ham, S. W. Nam, Performance and properties of anodes reinforced with metal oxide nanoparticles for

- molten carbonate fuel cells, *Journal of Power Sources* 370 (2017) 52–60.
- [47] M. E. Chelmehsara, J. Mahmoudimehr, Techno-economic comparison of anode-supported cathode-supported, and electrolyte-supported SOFCs, *International Journal of Hydrogen Energy* 43 (32) (2018) 15521–15530.
- [48] T. A. Prokop, K. Berent, H. Iwai, J. S. Szmyd, G. Brus, A three-dimensional heterogeneity analysis of electrochemical energy conversion in SOFC anodes using electron nanotomography and mathematical modeling, *International Journal of Hydrogen Energy* 43 (21) (2018) 10016–10030.
- [49] A. M. Abdalla, S. Hossain, A. T. Azad, P. M. I. Petra, F. Begum, S. G. Eriksson, A. K. Azad, Nanomaterials for solid oxide fuel cells: A review, *Renewable and Sustainable Energy Reviews* 82 (2018) 353–368.
- [50] K. Dzierzgowski, S. Wachowski, W. Gojtowska, I. Lewandowska, P. Jasiński, M. Gazda, A. Mielewczyk-Gryń, Praseodymium substituted lanthanum orthoniobate: Electrical and structural properties, *Ceramics International* 44 (7) (2018) 8210–8215.
- [51] L. J. M. J. Blomen, M. N. Mugerwa (Eds.), *Fuel Cell Systems*, Springer US, 1993.
- [52] F. Rodríguez, P. Sebastian, O. Solorza, R. PÉrez, Mo–Ru–W chalcogenide electrodes prepared by chemical synthesis and screen printing for fuel cell applications, *International Journal of Hydrogen Energy* 23 (11) (1998) 1031–1035.
- [53] A. D. Taylor, E. Y. Kim, V. P. Humes, J. Kizuka, L. T. Thompson, Inkjet printing of carbon supported platinum 3-D catalyst layers for use in fuel cells, *Journal of Power Sources* 171 (1) (2007) 101–106.
- [54] N. P. Kulkarni, Design and development of manufacturing methods for manufacturing of PEM fuel cell MEA's.
- [55] M. R. Somalu, N. P. Brandon, Rheological Studies of Nickel/Scandia-Stabilized-Zirconia Screen Printing Inks for Solid Oxide Fuel Cell Anode Fabrication, *Journal of the American Ceramic Society* 95 (4) (2011) 1220–1228.
- [56] M. Somalu, V. Yufit, I. Shapiro, P. Xiao, N. Brandon, The impact of ink rheology on the properties of screen-printed solid oxide fuel cell anodes, *International Journal of Hydrogen Energy* 38 (16) (2013) 6789–6801.
- [57] R. Baumann, A. Willert, F. Siegel, A. Kohl, Method for producing catalyst layers for fuel cells, *uS Patent App.* 13/322,472 (may 24 2012).
- [58] W. Wang, S. Chen, J. Li, W. Wang, Fabrication of catalyst coated membrane with screen printing method in a proton exchange membrane fuel cell, *International Journal of Hydrogen Energy* 40 (13) (2015) 4649–4658.
- [59] M. R. Somalu, A. Muchtar, W. R. W. Daud, N. P. Brandon, Screen-printing inks for the fabrication of solid oxide fuel cell films: A review, *Renewable and Sustainable Energy Reviews* 75 (2017) 426–439.
- [60] A. Jayakumar, S. Singamneni, M. Ramos, A. Al-Jumaily, S. Pethaiah, Manufacturing the Gas Diffusion Layer for PEM Fuel Cell Using a Novel 3D Printing Technique and Critical Assessment of the Challenges Encountered, *Materials* 10 (7) (2017) 796.
- [61] A. Nadar, A. M. Banerjee, M. Pai, R. Pai, S. S. Meena, R. Tewari, A. Tripathi, Catalytic properties of dispersed iron oxides Fe₂O₃/MO₂ (M = Zr Ce, Ti and Si) for sulfuric acid decomposition reaction: Role of support, *International Journal of Hydrogen Energy* 43 (1) (2018) 37–52.
- [62] E. Arato, E. Audasso, L. Barelli, B. Bosio, G. Discepoli, Kinetic modelling of molten carbonate fuel cells: Effects of cathode water and electrode materials, *Journal of Power Sources* 330 (2016) 18–27.
- [63] M. Peksen, Safe heating-up of a full scale SOFC system using 3D multiphysics modelling optimisation, *International Journal of Hydrogen Energy* 43 (1) (2018) 354–362.
- [64] E. El-Hay, M. El-Hameed, A. El-Fergany, Steady-state and dynamic models of solid oxide fuel cells based on Satin Bowerbird Optimizer, *International Journal of Hydrogen Energy* 43 (31) (2018) 14751–14761.
- [65] J. Milewski, M. Wołowicz, A. Miller, R. Bernat, A reduced order model of Molten Carbonate Fuel Cell: A proposal, *International Journal of Hydrogen Energy* 38 (26) (2013) 11565–11575.
- [66] M. Ławryńczuk, Towards Reduced-Order Models of Solid Oxide Fuel Cell, *Complexity* 2018 (2018) 1–18.
- [67] S. E. Shaheen, R. Radspinner, N. Peyghambarian, G. E. Jabbour, Fabrication of bulk heterojunction plastic solar cells by screen printing, *Applied Physics Letters* 79 (18) (2001) 2996–2998.